

CMS Internal Note

The content of this note is intended for CMS internal use and distribution only

21 January 2009

Material Budget in the Hadron Calorimeter

Sunanda Banerjee, Seema Sharma

Abstract

The detailed geometry information provided to the simulation software can be used to study the material budget of the detector components. In case of the hadron calorimeter, the material budget of the preceding absorber layers provides an estimation of sampling weights. A tool has been developed within the CMS software framework to study various aspects of material budget of the hadron calorimeter. The tool can also be used to validate the geometry description for subsequent releases.

1 Introduction

Information of material content in terms of number of radiation and/or interaction length is very useful in reconstructing tracks or clusters in a detector. For sampling calorimeters, the material traversed before a sensitive layer can be used to estimate the weight to be given to the energy deposit in that layer. The hadron calorimeter (HCAL) of CMS [1] is a sampling calorimeter of alternate layers of brass and plastic scintillators. The hadron calorimeter is divided into a barrel part (HB) covering the central part of the detector ($|\eta| < 1.39$) and two endcap regions (HE) covering the forward and the backward regions ($1.30 < |\eta| < 3.0$). There are also layers of scintillators behind the magnet coil which constitute the outer hadron calorimeter (HO). Very forward and backward region of the CMS detector are equipped with quartz fibres inside iron absorbers (HF) to measure forward going jets. Figure 1 shows a picture of the CMS detector with approximate position of the different components of the hadron calorimeter.

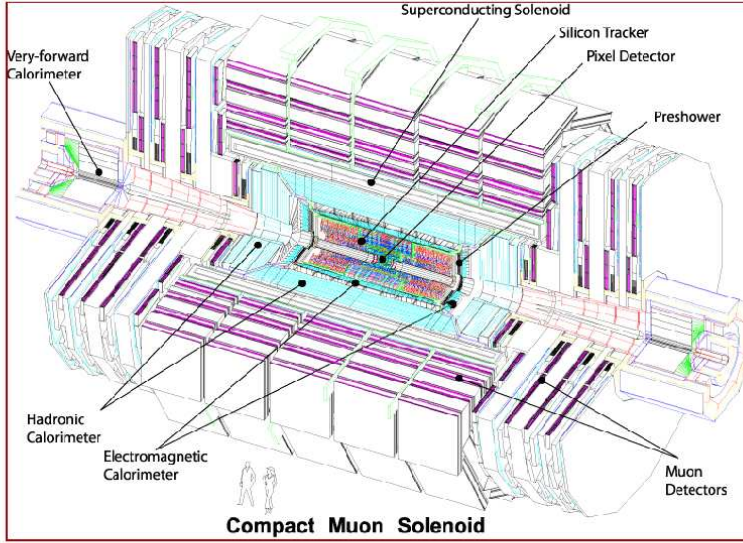


Figure 1: A perspective view of the CMS detector showing its different components.

The geometry of the entire CMS detector is described in the offline software framework CMSSW [2] with accurate information of position of the various components and also the material descriptions. This is crucial to simulate the response of the detector to the passage of particles produced. This description can be used to determine amount of material along a given direction in terms of radiation or interaction length.

The description is continuously improved with the information obtained from the construction and assembly centres of the detector. It is important to monitor the changes in the geometry information in subsequent releases of CMSSW. This radiographic information of number of radiation and interaction lengths along different direction can be used to monitor the changes in the geometry.

A tool has been developed within CMSSW framework to carry out this activity. Section 2 describes the method and the parameters used to get this information. Section 3 shows some of the results obtained from the tool. Some of the observations are explored in more detail in Section 4. The utilization of material budget information is discussed in Section 5 and Section 6 provides the summary of the report.

2 Methodology

A sample of events is produced each containing a single neutrino with direction randomly chosen with pseudo-rapidity (η) between -5.5 and 5.5 and azimuthal angle (ϕ) between 0 and 2π . These events are traced through the CMS detector setup. A *SimWatcher* class is set up which watches each step during propagation and keeps track of total lengths traversed in term of radiation and interaction lengths. If a sensitive detector layer of hadron

calorimeter is encountered, the traversed length is histogrammed for that layer as a function of η , ϕ of the neutrino. Tracking is continued till the neutrino leaves the detector setup or is beyond a region specified by a cylinder of given radius (R_{\max}) and half-length (Z_{\max}). Once the input file is exhausted, the entire set of profile histograms are written to a file and analyzed further using a ROOT macro. For each layer, three profile histograms are created. Two of them are one dimensional - one as a function of η and the other as a function of ϕ . The remaining one is a two dimensional profile histogram (function of η and ϕ).

A sample configuration file for running the CMSRUN job is provided as `test/runHcal_cfi.py` in the path *Validation/Geometry* of CMSSW and is given below:

```

import FWCore.ParameterSet.Config as cms

process = cms.Process("PROD")
#Geometry
#
process.load("Geometry.CMSCommonData.cmsIdealGeometryXML_cfi")
process.load("Geometry.TrackerNumberingBuilder.trackerNumberingGeometry_cfi")

#Magnetic Field
#
process.load("Configuration.StandardSequences.MagneticField_38T_cff")

# Detector simulation (Geant4-based)
#
process.load("SimG4Core.Application.g4SimHits_cfi")

process.RandomNumberGeneratorService = cms.Service("RandomNumberGeneratorService",
    moduleSeeds = cms.PSet(
        g4SimHits = cms.untracked.uint32(9876)
    )
)

process.MessageLogger = cms.Service("MessageLogger",
    destinations = cms.untracked.vstring('cout'),
    categories = cms.untracked.vstring('MaterialBudget'),
    cout = cms.untracked.PSet(
        default = cms.untracked.PSet(
            limit = cms.untracked.int32(0)
        ),
        MaterialBudget = cms.untracked.PSet(
            limit = cms.untracked.int32(-1)
        )
    )
)

process.source = cms.Source("MCFileSource",
    # The HepMC test File
    fileNames = cms.untracked.vstring('file:single_neutrino.random.dat')
)

process.maxEvents = cms.untracked.PSet(
    input = cms.untracked.int32(-1)
)

process.TFileService = cms.Service("TFileService",
    fileName = cms.string('matbdg_HCAL2.root')
)

```

```

process.p1 = cms.Path(process.g4SimHits)
process.g4SimHits.Generator.HepMCProductLabel = 'source'
process.g4SimHits.UseMagneticField = False
process.g4SimHits.Physics.type = 'SimG4Core/Physics/DummyPhysics'
process.g4SimHits.Physics.DummyEMPhysics = True
process.g4SimHits.Physics.CutsPerRegion = False
process.g4SimHits.Watchers = cms.VPSet(cms.PSet(
    MaterialBudgetHcal = cms.PSet(
        RMax      = cms.untracked.double(5.0),
        ZMax      = cms.untracked.double(14.0),
        HistoFile = cms.untracked.string('matbdg_HCAL.root'),
        NbinEta  = cms.untracked.int32(260),
        NbinPhi  = cms.untracked.int32(180),
        MaxEta   = cms.untracked.double(5.2),
        etaLow   = cms.untracked.double(-3.0),
        etaHigh  = cms.untracked.double(3.0)
    ),
    type = cms.string('MaterialBudgetHcal')
))

```

It uses the geometry configuration file `cmsIdealGeometryXML_cfi.py` from `Geometry/CMSCommonData/python` and a local input file `single_neutrino.random.dat` containing a number of single ν events. Such a file can be created using the configuration file `single_neutrino_cfi.py` from `Validation/Geoemtry/python`. The program utilizes the `SimWatcher` class `MATERIALBUDGETHCAL` with a specific set of parameter values. The root script `MatBudgetHcal.C` kept in the `test` sub-directory are equipped with several functions to provide one- (`etaPhiPlot`) or two- (`etaPhi2DPlot`) dimensional plots of material budget in term of total step lengths as well as number of interaction or radiation lengths. Also differential plots (`plotDiff`) can be made using the script.

3 Results

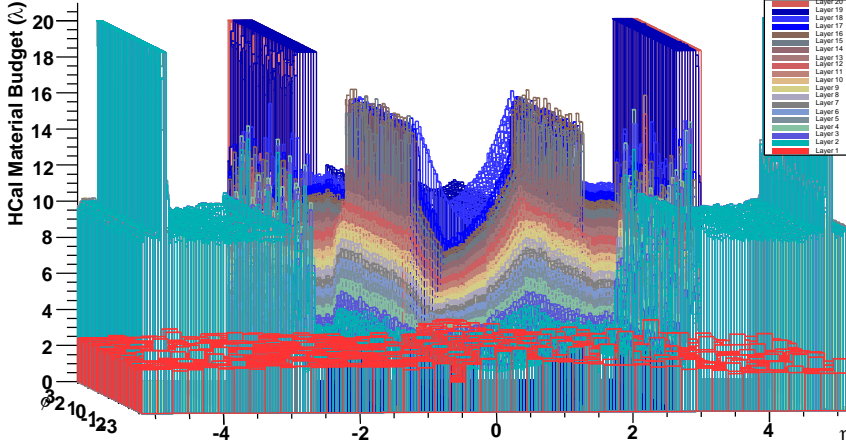


Figure 2: Material budget up to the last layers of CMS hadron calorimeter as a function of pseudo-rapidity, η and azimuthal angle, ϕ

Figure 2 shows the material budget up to the last layers of CMS hadron calorimeter as a function of pseudo-rapidity, η and azimuthal angle, ϕ . It shows an increase in number of total interaction length from 10.5 from the middle of the detector ($\eta \approx 0$) to 15.3 at the edge of the barrel hadron calorimeter ($\eta \approx 1.3$). In the endcap region, the last layer of scintillator is roughly behind 11 interaction length away from the interaction point. The forward hadron calorimeter puts up roughly 10 interaction lengths of absorber material. There are a few abnormally high spikes in the plot at η values in the range 2.64:3.00, 4.84:4.88 and 4.88:4.92. These η regions are looked into some detail

and discussed in Section 4. For a more clearer picture, the material budget plot as a function of pseudo-rapidity η for all values of ϕ is shown in Figure 3.

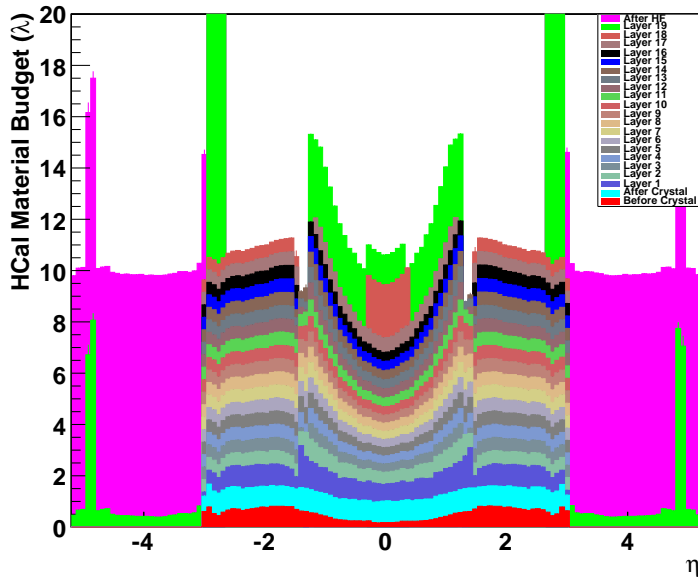


Figure 3: Material budget up to the last layers of CMS hadron calorimeter as a function of pseudo-rapidity, η averaged over all values of the azimuthal angle, ϕ

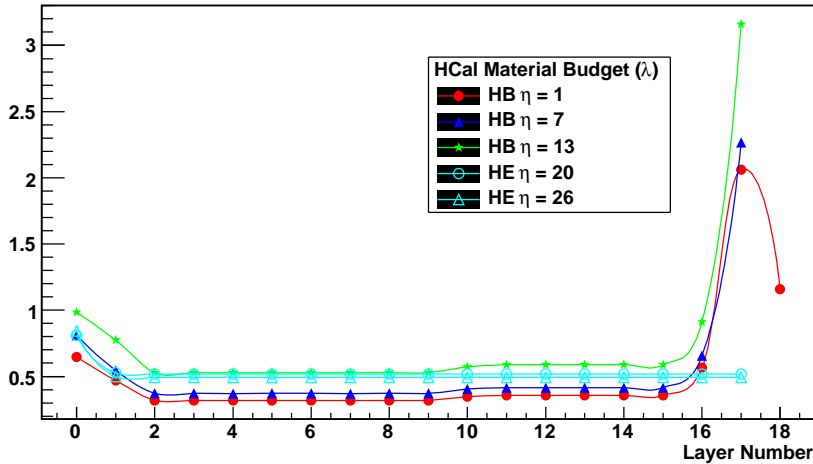


Figure 4: Material budget in term of number of interaction lengths in front of each layer of the calorimeter for several η towers.

Figures 4 and 5 show amount of material in terms of number of interaction and radiation lengths in front of each layer for several calorimeter towers corresponding to 3 towers in the barrel region (corresponding to $i\eta$ values of 1, 7 and 13) and 2 towers in the endcap region (corresponding to $i\eta$ values of 20 and 26). The first layer (layer 0) sees additional material ($\sim 0.65\lambda$ for $i\eta = 1$) which is due to the cooling, electronics and support material behind the crystals of the electromagnetic calorimeter. Layer 1 of the barrel calorimeter also sees some larger material budget ($\sim 0.47\lambda$ for $i\eta = 1$) due to the stainless steel structure at the front of the barrel wedge. The barrel towers show essentially 2 step-structure of absorber layers, one set is for layers 2-9 ($\sim 0.32\lambda$ for $i\eta = 1$) and the other is for layers 10-15 ($\sim 0.36\lambda$ for $i\eta = 1$). The material budget increases again for layer 16 due to the back structure of the wedge made out of stainless steel ($\sim 0.57\lambda$ for $i\eta = 1$). The last layers of the barrel towers show the effect of the outer hadron calorimeter which provides 2 layers for $i\eta = 1-4$ and only 1 layer for $i\eta = 5-15$. The number of

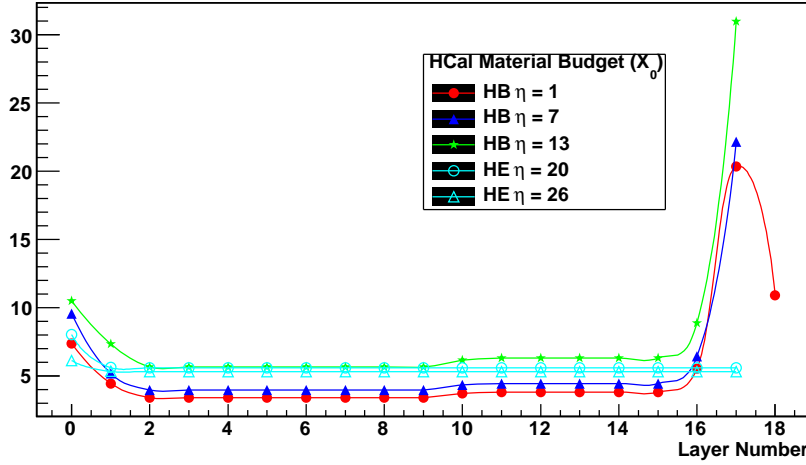


Figure 5: Material budget in term of number of radiation lengths in front of each layer of the calorimeter for several η towers.

interaction lengths in front of different towers of the barrel calorimeter is summarized in Table 1.

$i\eta$	η	# of interaction lengths before						
		layer 0	layer 1	layers 2-9	layers 10-15	layer 16	layer 17	layer 18
1	0.043	0.648	0.468	0.319	0.356	0.565	2.062	1.160
2	0.131	0.720	0.472	0.321	0.359	0.570	2.076	1.172
3	0.217	0.734	0.479	0.326	0.364	0.579	2.104	1.190
4	0.304	0.751	0.490	0.334	0.372	0.592	2.077	0.870
5	0.391	0.694	0.504	0.343	0.383	0.608	1.966	
6	0.479	0.753	0.522	0.356	0.397	0.630	2.258	
7	0.566	0.811	0.545	0.371	0.414	0.657	2.266	
8	0.652	0.828	0.572	0.389	0.434	0.690	2.325	
9	0.740	0.803	0.601	0.410	0.457	0.724	2.463	
10	0.827	0.902	0.637	0.434	0.484	0.768	2.597	
11	0.913	0.915	0.676	0.461	0.514	0.814	2.785	
12	1.000	0.993	0.721	0.492	0.549	0.867	2.954	
13	1.090	0.984	0.774	0.527	0.588	0.912	3.159	
14	1.170	1.075	0.828	0.565	0.630	0.473	3.103	
15	1.260	1.125	0.890	0.608	0.639		3.399	

Table 1: Amount of absorber material in number of interaction lengths in front of different layers for various towers of the barrel hadron calorimeter

The endcap towers show very smooth layer-wise breakup. The only non-uniformity is in the layer 0 which is again due to the material behind the endcap electromagnetic calorimeter. The number of interaction lengths in front of different towers of the endcap calorimeter is summarized in Table 2.

The crystals and the tracker material provide some additional material before the hadron calorimeter. Figure 6 shows amount of material in front and behind the crystal. The tracker and the crystal provide additional $1-1.2 \lambda$ material (apart from the material between ECAL and HCAL). The material in front of the first HCAL layer at η values (1.34:1.38) shows a spike of nearly $5\lambda_{\text{Int}}$ and this is investigated in the section 4.

Figure 7 shows material budget in term of number of interaction lengths as a function of pseudo-rapidity η in front of the hadron calorimeter, till the last layer of HB and HE and till the last layer of HO. The outer hadron calorimeter typically adds 2 interaction lengths to the system so that the entire barrel region has a minimum of 10 interaction lengths for all η values.

The software package can be used to validate the geometry definition in a given version. A major revision of the geometry was made between the CMSSW versions 1_5_1 and 1_7_0. The function `printTable` within the root script

$i\eta$	η	# of interaction lengths before		
		layer 0	layer 1	layers 2-17
18	1.52	0.340	0.509	0.533
19	1.61	0.799	0.534	0.525
20	1.70	0.811	0.526	0.519
21	1.79	0.853	0.521	0.513
22	1.88	0.851	0.516	0.508
23	1.99	0.825	0.511	0.504
24	2.11	0.874	0.507	0.499
25	2.25	0.864	0.504	0.496
26	2.41	0.844	0.500	0.493
27	2.58	0.805	0.498	0.491
28	2.83	0.580	0.495	0.488
29	2.91	0.602	0.495	0.488
30	3.05	0.137	0.494	0.485

Table 2: Amount of absorber material in number of interaction lengths in front of different layers for various towers of the endcap hadron calorimeter

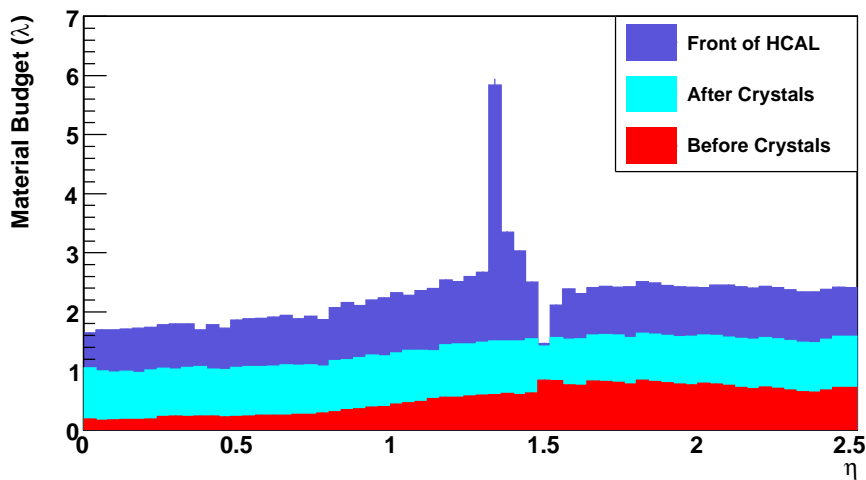


Figure 6: Material budget in term of number of interaction lengths in front and behind the crystal and in front of the first layer of hadron calorimeter as a function of pseudo-rapidity η .

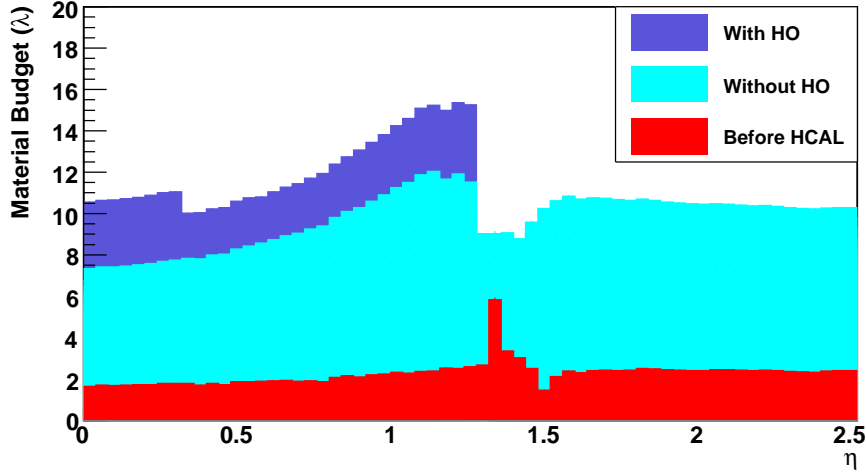


Figure 7: Material budget in term of number of interaction lengths as a function of pseudo-rapidity η in front of the hadron calorimeter, till the last layer of HB and HE and till the last layer of HO.

MatBudgetHcal.C has been used to provide the difference between the two versions of the geometry:

Lambda::Tower	0	Layer	0	Old	1.629	New	1.658	Diff	0.01766
Lambda::Tower	1	Layer	0	Old	1.684	New	1.706	Diff	0.01288
Lambda::Tower	2	Layer	0	Old	1.728	New	1.752	Diff	0.01366
Lambda::Tower	3	Layer	0	Old	1.785	New	1.809	Diff	0.01324
Lambda::Tower	4	Layer	0	Old	1.761	New	1.787	Diff	0.0144
Lambda::Tower	5	Layer	0	Old	1.786	New	1.813	Diff	0.01526
Lambda::Tower	6	Layer	0	Old	1.902	New	1.927	Diff	0.01305
Lambda::Tower	7	Layer	0	Old	1.928	New	1.957	Diff	0.01487
Lambda::Tower	8	Layer	0	Old	1.868	New	1.895	Diff	0.01409
Lambda::Tower	9	Layer	0	Old	2.027	New	2.05	Diff	0.01114
Lambda::Tower	10	Layer	0	Old	2.107	New	2.145	Diff	0.01774
Lambda::Tower	11	Layer	0	Old	2.293	New	2.332	Diff	0.01693
Lambda::Tower	12	Layer	0	Old	2.317	New	2.414	Diff	0.04083
Lambda::Tower	13	Layer	0	Old	2.409	New	2.517	Diff	0.04371
Lambda::Tower	14	Layer	0	Old	2.531	New	2.638	Diff	0.04156
Lambda::Tower	15	Layer	0	Old	2.862	New	2.982	Diff	0.04122
Lambda::Tower	15	Layer	10	Old	0.3494	New	0.3659	Diff	0.04623
Lambda::Tower	16	Layer	0	Old	2.587	New	2.758	Diff	0.06404
Lambda::Tower	16	Layer	12	Old	0.0212	New	0.159	Diff	1.529
Lambda::Tower	16	Layer	13	Old	0.2704	New	0.3256	Diff	0.1853
Lambda::Tower	17	Layer	0	Old	1.546	New	1.798	Diff	0.1508
Lambda::Tower	17	Layer	16	Old	0.6128	New	0.6478	Diff	0.0555
Lambda::Tower	18	Layer	0	Old	1.859	New	2.359	Diff	0.2372
.....									
.....									

4 Blind Regions

The peak in the material in front of the first active layer in HCAL at η around 1.36 is investigated by printing the information of all geometry volumes traversed by the particle between the crystal and the first sensitive layer of HCAL. This η region corresponds to the gap between the barrel and the endcap calorimeter. There are two scenarios for the particles crossing the detector at this solid angle. In the first scenario, the particles cross the tracker cables and connectors after getting past the ECAL material behind the crystal. In this scenario, the track traverses a total of $3.24 \cdot \lambda_{\text{Int}}$ material before reaching the the first sensitive layer of HCAL.

EBRY_16	(PbWO4)	L/Lambda 1.11095/0.852329
ECLR_16	(Air)	L/Lambda 7.11388e-06/1.96328
EHAWR	(Air)	L/Lambda 9.16774e-05/1.96329
EGRID	(Aluminium)	L/Lambda 0.157283/1.96338
EHAWR	(Air)	L/Lambda 6.91665e-06/2.12066
ESPM	(Air)	L/Lambda 6.8115e-05/2.12067
EBCOOL4	(Air)	L/Lambda 1.72286e-05/2.12074
EMBL1_4	(Air)	L/Lambda 2.87144e-06/2.12075
EMBL2_4	(Aluminium)	L/Lambda 0.0136211/2.12076
EMBL3_4	(G10)	L/Lambda 0.00850011/2.13438
EMBL4_4	(Silicon)	L/Lambda 0.0044606/2.14288
EMBL5_4	(Copper)	L/Lambda 0.00130667/2.14734
EVFE_2	(Aluminium)	L/Lambda 0.000430284/2.14864
EVFE_3	(G10)	L/Lambda 0.00479154/2.14908
EVFE_4	(Silicon)	L/Lambda 0.00251445/2.15387
EVFE_5	(Copper)	L/Lambda 0.000736575/2.15638
EBCOOL4	(Air)	L/Lambda 2.15279e-05/2.15712
EVFE_5	(Copper)	L/Lambda 0.000736575/2.15714
EVFE_4	(Silicon)	L/Lambda 0.00251445/2.15788
EVFE_3	(G10)	L/Lambda 0.00479154/2.16039
EVFE_2	(Aluminium)	L/Lambda 0.0095978/2.16518
EVFE_1	(Air)	L/Lambda 1.61864e-06/2.17478
EBCBAR	(Aluminium)	L/Lambda 0.0105428/2.17478
EBCBSS	(StainlessSteel)	L/Lambda 0.00107033/2.18532
EBCBWA	(Water)	L/Lambda 0.000837281/2.18639
EBCBSS	(StainlessSteel)	L/Lambda 0.00107033/2.18723
EBCBAR	(Aluminium)	L/Lambda 0.0105428/2.1883
EVFE_1	(Air)	L/Lambda 1.61864e-06/2.19884
EVFE_2	(Aluminium)	L/Lambda 0.0095978/2.19885
EVFE_3	(G10)	L/Lambda 0.00479154/2.20844
EVFE_4	(Silicon)	L/Lambda 0.00251445/2.21324
EVFE_5	(Copper)	L/Lambda 0.000736575/2.21575
EBCOOL4	(Air)	L/Lambda 0.000136451/2.21649
ESPM	(Air)	L/Lambda 5.3415e-05/2.21662
EGRL7	(Aluminium)	L/Lambda 0.0590634/2.21668
ESPM	(Air)	L/Lambda 8.09318e-07/2.27574
EPPSI	(Silicon)	L/Lambda 0.0356799/2.27574
EPPCU	(Copper)	L/Lambda 0.0653337/2.31142
EPPWA	(Water)	L/Lambda 0.13503/2.37675
EPPSS	(StainlessSteel)	L/Lambda 0.1225/2.51178
ESPM	(Air)	L/Lambda 6.55564e-05/2.63428
EBAR	(Air)	L/Lambda 1.63073e-06/2.63435
ECAL	(Air)	L/Lambda 2.04819e-05/2.63435
Tracker_PP1_Cables	(Tk_Cables)	L/Lambda 0.0819466/2.63437
Tracker_PP1_Connectors	(Tk_Connectors_PP1)	L/Lambda 0.0154022/2.71632
HCal	(Air)	L/Lambda 0.000156263/2.73172
HTC1	(Tk_square_bundles)	L/Lambda 0.074549/2.73188
HCal	(Air)	L/Lambda 0.000176467/2.80643
HBLayer2	(Brass)	L/Lambda 0.427948/2.8066
HBLayer2In2	(Air)	L/Lambda 7.23224e-06/3.23455
HBLayer2In2Plastic_1	(Polyethylene)	L/Lambda 0.00571921/3.23456
HBScintillatorLayer2In2	(Scintillator)	L/Lambda 0.0107607/3.24028

In a second scenario, the particle sees more material before reaching the first sensitive layer of HCAL. Here the particle misses sensitive layers in the barrel detector but traverses a part of the absorber there. Total amount of material traversed in this scenario could be as high as $5.72 \cdot \lambda_{\text{Int.}}$

EBRY_16	(PbWO4)	L/Lambda 0.895276/0.991478
---------	---------	----------------------------

EAPD_16	(Silicon)	L/Lambda 1.09682e-05/1.88675
ECLR_16	(Air)	L/Lambda 7.10623e-06/1.88676
EHAWR	(Air)	L/Lambda 6.82042e-05/1.88677
EGRID	(Aluminium)	L/Lambda 0.158536/1.88684
EHAWR	(Air)	L/Lambda 7.04465e-06/2.04538
ESPM	(Air)	L/Lambda 8.28e-05/2.04538
EBCOOL4	(Air)	L/Lambda 1.74207e-05/2.04547
EMBL1_4	(Air)	L/Lambda 2.90346e-06/2.04548
EMBL2_4	(Aluminium)	L/Lambda 0.013773/2.04549
EMBL3_4	(G10)	L/Lambda 0.0085949/2.05926
EMBL4_4	(Silicon)	L/Lambda 0.00451035/2.06785
EMBL5_4	(Copper)	L/Lambda 0.00132124/2.07236
EVFE_3	(G10)	L/Lambda 0.00262708/2.07369
EVFE_4	(Silicon)	L/Lambda 0.00250804/2.07631
EVFE_5	(Copper)	L/Lambda 0.000734697/2.07882
EBCOOL4	(Air)	L/Lambda 0.000136103/2.07956
ESPM	(Air)	L/Lambda 5.32788e-05/2.07969
EGRL7	(Aluminium)	L/Lambda 0.0589128/2.07974
ESPM	(Air)	L/Lambda 8.07254e-07/2.13866
EPPG10	(G10)	L/Lambda 0.08574/2.13866
EPPSI	(Silicon)	L/Lambda 0.0451035/2.2244
EPPCU	(Copper)	L/Lambda 0.0660622/2.2695
EPPWA	(Water)	L/Lambda 0.136535/2.33556
EPPSS	(StainlessSteel)	L/Lambda 0.118658/2.4721
EBAR	(Air)	L/Lambda 1.62657e-06/2.59076
ECAL	(Air)	L/Lambda 2.04297e-05/2.59076
Tracker_PP1_Cables	(Tk_Cables_PP1)	L/Lambda 0.0817377/2.59078
Tracker_PP1_Connectors	(Tk_Connectors_PP1)	L/Lambda 0.0282749/2.67252
HCal	(Air)	L/Lambda 0.000101024/2.70079
HHC1	(Air)	L/Lambda 0.000186395/2.70089
HCal	(Air)	L/Lambda 0.000178432/2.70108
HBLayer2	(Brass)	L/Lambda 0.056441/2.70126
HBLayer2In1	(Air)	L/Lambda 2.77886e-05/2.75777
HBLayer2	(Brass)	L/Lambda 0.376273/2.75773
HBLayer3	(Brass)	L/Lambda 0.25712/3.134
HBLayer3In1	(Air)	L/Lambda 2.77886e-05/3.39112
HBLayer3	(Brass)	L/Lambda 0.376273/3.39115
HBLayer4	(Brass)	L/Lambda 0.25712/3.76742
HBLayer4In1	(Air)	L/Lambda 2.77886e-05/4.02454
HBLayer4	(Brass)	L/Lambda 0.376273/4.02457
HBLayer5	(Brass)	L/Lambda 0.25712/4.40084
HBLayer5In1	(Air)	L/Lambda 2.77886e-05/4.65796
HBLayer5	(Brass)	L/Lambda 0.376273/4.65799
HBLayer6	(Brass)	L/Lambda 0.25712/5.03426
HBLayer6In1	(Air)	L/Lambda 2.77886e-05/5.29138
HBLayer6	(Brass)	L/Lambda 0.225788/5.29141
HCal	(Air)	L/Lambda 2.69271e-07/5.5172
HHC1	(Air)	L/Lambda 0.000263236/5.5172
HCal	(Air)	L/Lambda 0.000232885/5.51746
HEPart3	(Brass)	L/Lambda 0.205489/5.5177
HEPart3Layer04PhilAir	(Air)	L/Lambda 1.62657e-06/5.72318
HEPart3Layer04Phil	(Polyethylene)	L/Lambda 0.00265295/5.72319
HEScintillatorPart3Layer04Phil	(Scintillator)	L/Lambda 0.00605035/5.72584

The peak in the material budget plot at η around 2.8 is examined by printing the information of all the layers traversed by a ν track emitted at that direction. The particle will go through parts of tracker, endcap electromagnetic and hadron calorimeter, support material of the forward muon detectors before reaching the forward hadron calorimeter. The structure of material between endcap and forward hadron calorimeter is shown in Figure 8 and

step-wise accumulation of interaction length is shown below:

HEPart5Layer18Phi1	(Polyethylene)	L/Lambda 0.00233478/10.2641
HEPart5Layer18Phi1Air	(Air)	L/Lambda 1.43149e-06/10.2665
HEBack	(H_Brass)	L/Lambda 0.146801/10.2665
SupportTubeForHE	(StainlessSteel)	L/Lambda 7.33903/10.4133
ME	(M_F_Air)	L/Lambda 0.000118333/17.7523
YN12p_b	(AISI-1018-Steel)	L/Lambda 0.591045/17.7524
YN12p_c	(AISI-1018-Steel)	L/Lambda 1.95045/18.3435
YE1p_a	(AISI-1018-Steel)	L/Lambda 4.19642/20.2939
YE12	(AISI-1018-Steel)	L/Lambda 3.2212/24.4903
YE2p_a	(AISI-1018-Steel)	L/Lambda 4.19642/27.7115
YE23	(AISI-1018-Steel)	L/Lambda 3.22179/31.9079
YE3p_a	(AISI-1018-Steel)	L/Lambda 2.12717/35.1297
YE34	(AISI-1018-Steel)	L/Lambda 3.22179/37.2569
ShieldingME4	(AISI-1018-Steel)	L/Lambda 0.442693/40.4787
ShieldingBoronPoly_1_ME	(Boron Polyethyl.)	L/Lambda 0.150975/40.9214
ME	(M_F_Air)	L/Lambda 7.1044e-06/41.0724
CMSE	(Air)	L/Lambda 0.000414417/41.0724
HVQF	(Air)	L/Lambda 7.15746e-07/41.0728
HVQX	(Iron)	L/Lambda 7.85886/41.0728
HVQF	(Air)	L/Lambda 0.000277571/48.9316
CMSE	(Air)	L/Lambda 0.0190826/48.9319

Thus particles see the support tube of HE as well the forward yoke material of YE1/YE2/YE3 before it reaches the top of HF. This region of HF will hardly be useful for measurement of hadron jets.

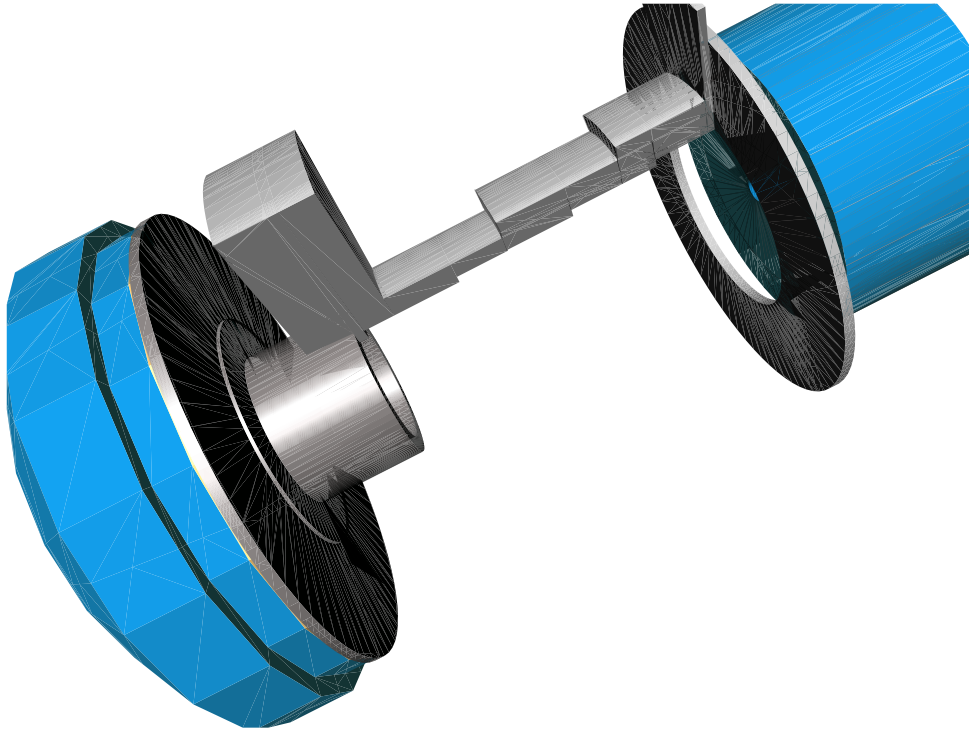


Figure 8: View of the CMS detector showing boundaries of the endcap and the forward hadron calorimeter and some of the components in-between which comprise parts of support structure of endcap muon detector.

Similarly the structure at $\eta = 4.85$ is examined by looking into the traversed detector components by a particle emitted at that direction. The particle will see parts of stainless steel structure in the conical part of the beam pipe between 3.388 m and 10.539 m (defined by BeamTube6) and will cross material equivalent to $8.69 \lambda_{\text{Int}}$ before reaching the front face of HF. The beam pipe structure of the section BeamTube6 is shown in Figure 9. The

break-up of the contribution to $\ell/\lambda_{\text{Int}}$ in different part of the setup is given below.

BEAM	(Air)	L/Lambda 0.000234375/0.438096
BeamVacuum6	(Vacuum)	L/Lambda 2.20027e-17/0.43833
BEAM	(Air)	L/Lambda 0.00243421/0.43833
BeamTube6	(StainlessSteel)	L/Lambda 4.99782/0.440764
BeamVacuum6	(Vacuum)	L/Lambda 2.04462e-16/5.43858
BeamTube6	(StainlessSteel)	L/Lambda 3.24556/5.43858
BEAM	(Air)	L/Lambda 0.000310098/8.68414
CMSE	(Air)	L/Lambda 0.00518537/8.68445
HVQF	(Air)	L/Lambda 7.10227e-07/8.68964
HVQX	(Iron)	L/Lambda 9.7074/8.68964
HVQF	(Air)	L/Lambda 7.10227e-07/18.397



Figure 9: Sections of the beam pipe structure (a) between 3.388 m and 10.539 m and (b) between 1.940 m and 2.719 m. The conical structures have pointing geometry corresponding to η value of 4.85.

A particle traversing at $\eta = 4.88$ will see parts of stainless steel structure in the conical part of the beam pipe between 1.94 m (start of the structure called BeamTube3) till 10.54 m (end of section BeamTube6) and crosses material equivalent to $27.75 \lambda_{\text{Int}}$ before reaching the front face of HF. The beam pipe structure from 1.94 m to 10.539 m is shown in 4 parts in Figures 9 and 10. The step-wise contribution to cumulative interaction length of such a particle is given below:

BeamTube2	(StainlessSteel)	L/Lambda 0.201904/5.44758e-16
BeamTube3	(StainlessSteel)	L/Lambda 4.70368/0.201904
BeamTube4	(StainlessSteel)	L/Lambda 2.39394/4.90558
BeamTube5	(StainlessSteel)	L/Lambda 0.173312/7.29953
BEAM	(Air)	L/Lambda 1.87306e-05/7.47284
BeamVacuum5	(Vacuum)	L/Lambda 2.20025e-17/7.47286
BEAM	(Air)	L/Lambda 0.000234374/7.47286
BeamVacuum6	(Vacuum)	L/Lambda 2.20025e-17/7.47309
BEAM	(Air)	L/Lambda 2.69885e-05/7.47309
BeamTube6	(StainlessSteel)	L/Lambda 8.7264/7.47312
BeamVacuum6	(Vacuum)	L/Lambda 7.27825e-16/16.1995
BeamTube6	(StainlessSteel)	L/Lambda 11.5466/16.1995
CMSE	(Air)	L/Lambda 0.00246017/27.7461
HVQF	(Air)	L/Lambda 7.10223e-07/27.7485
HVQX	(Iron)	L/Lambda 9.70733/27.7485
HVQF	(Air)	L/Lambda 7.10223e-07/37.4559

Thus the conical part of the beam tube structure provides a shadow to part of the HF and spoil the energy measurements in that region.

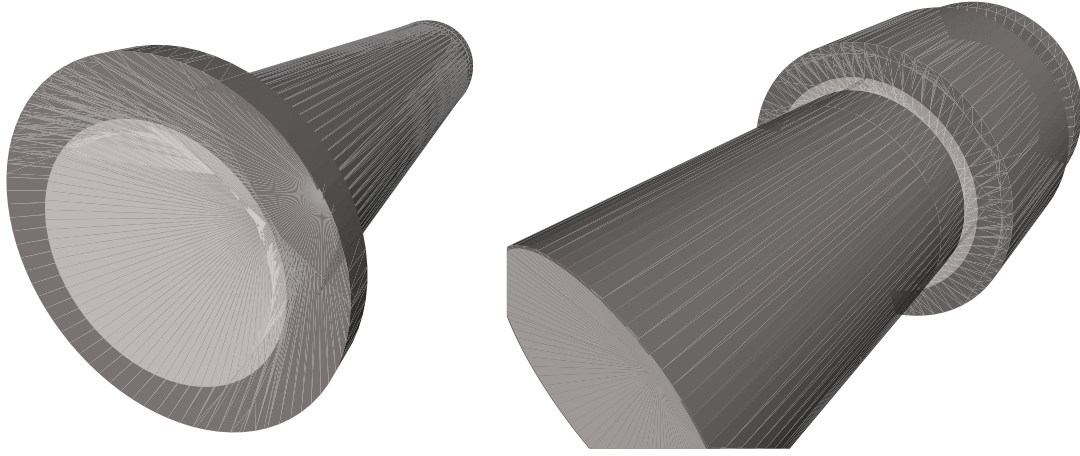


Figure 10: Sections of the beam pipe structure (a) between 2.719 m and 3.12 m and (b) between 3.12 m and 3.3876 m.

5 Usage of Material Budget Information

The material preceding a sensitive layer will provide the sampling factor for a given depth. As an example, let us consider the tower at $i\eta = 7$. Here the part for HB consists of 17 layers of average absorber material of $0.46\lambda_{\text{Int}}$ while the outer hadron calorimeter corresponds to $2.27\lambda_{\text{Int}}$. The relative sampling thickness of scintillator provides roughly 2.5 times more light in HO. This will thus indicate roughly a weight factor of 2 ($\equiv 2.27/(0.46*2.5)$) for energy measured in HO with respect to the energy measured in HB.

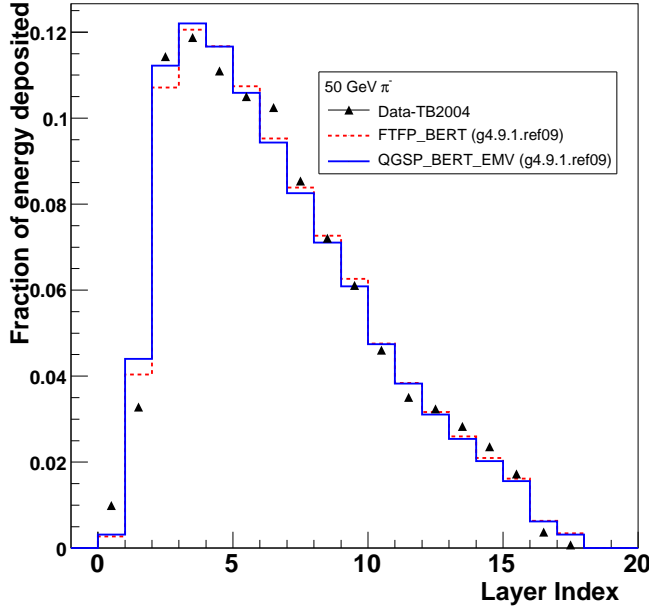


Figure 11: Longitudinal shower profile for 50 GeV/c π^- beam in the hadron calorimeter compared to Monte Carlo predictions from different Geant4 shower models.

The material budget information is also used in measuring the longitudinal shower profile of hadrons in the hadron calorimeter. The energy measured in each layer is weighted by the inverse of the material budget to generate the longitudinal shower profile. The shower profiles, thus measured in real as well as simulated data, are compared in Figure 11 for 50 GeV/c π^- beam. As can be seen from the figure, the shower profile shows a smooth dependence on the layer number with the shower peak at the layer # 3. Data and Monte Carlo expectations show very similar shower shapes.

6 Summary

A tool has been developed with the CMSSW software frame work to study the material budget of the hadron calorimeter. This can be used to study detailed feature of energy measured by the hadron calorimeter as well specific features like sampling weights or longitudinal shower profiles.

The tool can also be used to validate the geometry description of the hadron calorimeter and can monitor the evolution of geometry description for subsequent CMSSW releases.

References

- [1] CMS Technical Proposal, CERN/LHCC 94-38, LHCC/P1, December 15, 1994.
- [2] CMSSW: <http://twiki.cern.ch/twiki/bin/view/CMS/WorkBook>